Caudatin targets TNFAIP1/NF-κB and cytochrome *c*/caspase signaling to suppress tumor progression in human uterine cancer

ZHI-WEN TAN[1,6*], SHUN XIE[1*], SI-YANG HU[1], TAO LIAO[1], PAN LIU[1], KE-HONG PENG[2,3], XIN-ZHOU YANG[1], ZHI-LI HE[1,5], HONG-YAN TANG[1], YUAN CUI[1], XIAO-NING PENG[4], JIAN ZHANG[1] and CHANG ZHOU[1]

[1]Key Laboratory of Protein Chemistry and Developmental Biology of State Education Ministry of China, College of Life Science, Hunan Normal University, Changsha, Hunan 410081; [2]Department of Gynecological Oncology, Hunan Cancer Hospital; [3]The Affiliated Cancer Hospital of Xiangya School of Medicine, Central South University; [4]College of Medicine, Hunan Normal University, Changsha, Hunan 410013; [5]Department of Hepatobiliary Surgery, Hunan Provincial People's Hospital, Changsha, Hunan, Hunan 410005; [6]Changsha Blood Center, Changsha, Hunan 410000, P.R. China

Received May 26, 2016; Accepted July 18, 2016

DOI: 10.3892/ijo.2016.3662

Abstract. Caudatin, a C-21 steroidal glycoside isolated from Chinese herbs, has a long history of use for the treatment of multiple diseases, including cancers. However, the precise mechanisms of actions of caudatin in human uterine cancer cells remain unclear. In this study, we investigated the molecular mechanisms by which caudatin inhibits cell growth in human cervical carcinoma cell line (HeLa) and endometrial carcinoma cell line (HEC-1A). Treatment with caudatin promoted cell morphology change, inhibited cell proliferation, colony formation, migration and spheroid formation, and induced cell apoptosis. Our results showed that the expression of tumor necrosis factor; α-induced protein 1 (TNFAIP1) was downregulated in uterine cancer cells and tissues compared to paired adjacent non-tumor uterine tissues. Further molecular mechanism study showed that caudatin can directly regulate TNFAIP1 expression in a concentration-dependent manner and also associated with the downregulation of NF-κB and upregulation of BAX/BcL-2 ratio and caspase-3. Moreover, we found that overexpression of TNFAIP1 inhibits the growth and invasion, and induces apoptosis in uterine cancer cells through inhibition of the NF-κB pathway, suggesting that TNFAIP1 may act as a potential therapeutic target for the treatment of cancer. We found that caudatin inhibited tumorigenicity and upregulated TNFAIP1 *in vivo*. Taken together, caudatin impacts on cell proliferation, migration and apoptosis of uterine cancer cells by regulating several carcinogenesis-related processes, including a novel mechanism involving the targeting of TNFAIP1/NF-κB signaling. Our findings provide new insights into understanding the anticancer mechanisms of caudatin in human uterine cancer therapy.

Correspondence to: Professor Chang Zhou, Key Laboratory of Protein Chemistry and Developmental Biology of State Education Ministry of China, College of Life Science, Hunan Normal University, Lushan South Road 36, Changsha, Hunan 410081, P.R. China
E-mail: zhouchang1972@126.com

*Contributed equally

Key words: caudatin, tumor necrosis factor, α-induced protein 1, human uterine cancer cell

Introduction

Uterine cancer is one of the most common malignancies and the second leading cause of cancer-related mortality worldwide in women. Worldwide each year 370,000 women develop uterine cancer and 200,000 die due to the disease (1,2). The incidence and mortality of uterine cancer in China accounts for ~1/3 of the whole world. The age distribution of this disease shows a peak between 35 and 39 years and a second peak between 60 and 64 years, the average age at first diagnosis has decreased to 52.2 years in China (3), while the incidence of invasive uterine cancer in China has increased in young women within the past few years (4). Despite recent advances in combining surgery, chemotherapy and radiotherapy no effective targeting therapy is available for uterine cancer, unfortunately, while some patients are eligible for curative treatment, recurrence is a frequent issue for many patients after tumor ablation (5). Accordingly, an urgent need exists to identify new therapeutic agents for the treatment of uterine cancer in clinical practice.

Chinese herbs have been used widely and successfully for centuries in treating different kinds of diseases. Natural products occupy a very important position in the area of cancer chemotherapy due to their excellent pharmacological activities and low toxicity (6-8). C-21 steroidal glycosides is one species of important biological active compounds widely found in the plants of the *Asclepiadaceae* family, which

has been shown to effectively remove hydroxyl radicals and oxygen-free radicals, regulating immunity, and protecting liver and gastric cells (9-11). Caudatin, a C-21 steroidal glycoside, is mainly isolated from the traditional Chinese medicine 'baishouwu', which was the root tuber of *Cynanchum auriculatum* Royle ex Wight. It has been reported that the antitumor effect of caudatin has been shown to exhibit anti-proliferation effects against cancer cells of different origins, including glioblastoma, lung, gastric, and liver cancer (12-16). In our previous studies, caudatin induced apoptosis of AGS cells or the HGC-27 cell line (14). Wang *et al* found that caudatin had an inhibitory activity on the secretion of HBsAg and HBV DNA replication (17). Furthermore, caudatin as a prospective anti-HCC drug with the mechanism of inhibiting cell proliferation and inducing cell apoptosis has been reported (18). Although evidence of antitumor effects of caudatin is expanding, uncertainty of the mechanisms of caudatin in uterine cancer still remains. Yet, there is no report concerning the effects of caudatin on uterine cancer, and the underlying mechanisms are not well documented. Up to now, the pharmacokinetics of caudatin in uterine carcinoma model animals remains unclear.

TNFAIP1 is an immediate-early response gene of endothelium induced by TNFα and IL-6. It may play roles in DNA synthesis, DNA repair, cell apoptosis and human diseases (19). TNFAIP1 has been identified to be highly expressed in Alzheimer's disease brains and hepatitis B virus, and is associated with diabetic nephropathy (20). Interestingly, TNFAIP1 is also abnormally expressed in gastric cancer, breast cancer, osteosarcoma, and cervical cancer, but little is known about its potential function in malignant disease (21-26). TNFAIP1 was highly expressed in normal cell lines while it was lowly expressed in cancer cell lines (27). Indeed, TNFAIP1 elicited proapoptotic activity, and co-expression of TNFAIP1 and RhoB markedly increased apoptosis in HeLa cells (28). TNFAIP1 and KCTD10 suppressed the transcriptional activities of NF-κB (29). We found that downregulation of TNFAIP1 is correlated with enhanced tumorigenicity, enhanced metastatic potential and poor prognosis in gastric cancer (23). Better understanding of the mechanism of action of TNFAIP1 is crucial in the development of new uterine tumor treatments.

The aims of this study were to determine effects of caudatin on proliferation, migration and apoptosis in HeLa and HEC-1A cells and to investigate its molecular mechanisms of action.

Materials and methods

Cell culture and transfection. The human cervical carcinoma cell line (HeLa) and endometrial carcinoma cell line (HEC-1A) were obtained from the Cell Bank of the Chinese Academy of Sciences (China). Cells were cultured in Dulbecco's modified Eagle's medium (DMEM; Hyclone) and F-12 (hyclone) supplemented with 10% FBS,100 U/ml penicillin, 100 U/ml streptomycin. All cells were grown at 37˚C in a humidified atmosphere with 5% CO_2 and passaged using 0.2% (w/v) trypsin and 0.1% (w/v) EDTA. The pCMV-Myc-TNFAIP1 and pCMV-Myc vectors that were used in this study were purchased from Clontech. All transfections were carried out using Lipofectamine 2000 (Invitrogen, USA), according to the manufacturer's instructions.

Clinical specimens. Fresh human cervical carcinoma and adjacent non-tumor tissue samples were obtained from the Department of Gynecologic Tumor, Hunan Cancer Hospital, Changsha, China. After surgical resection, the fresh tissue samples were immediately immersed in RNAlater (Ambion Inc., USA) and stored at room temperature 3-4 h; the samples were then frozen at -80˚C until RNA extraction. The samples were classified according to World Health Organization criteria published in 2000. All patients signed consent forms and the study protocol was approved by the Committee on Human Rights in Research of the Ethics Committee of the College of Life Science, Hunan Normal University, Changsha, China.

Reagents and antibodies. Caudatin was purchased from the Shenzhen Medherb Biotechnology Co., Ltd. (Shenzhen, China) and dissolved with 100% dimethyl sulfoxide (DMSO) (concentration of the stock solution, 10 mmol/l). Antibodies to Bcl-2, cytochrome *c* (Cyt-*c*), Caspase-9, Caspase-3, PARP and NFκB were obtained from Santa Cruz Biotechnology (Santa Cruz, CA, USA). β-actin antibody was purchased from GenScript, Inc. (Piscataway, NJ, USA), Antibody against Bax was purchased from Proteintech (USA) and antibody against TNFAIP1 was custom made from signalway antibody (Signalway Antibody LLC, USA).

RNA extraction and real-time PCR analysis. Total RNA was extracted using TRIzol reagent (Invitrogen) according to the manufacturer's instructions. Reverse transcription was reverse-transcribed by using the RevertAid First Strand cDNA Synthesis kit (Thermo Scientific, USA) with 1 μg total RNA, according to the manufacturer's instructions. Quantitative real-time PCR (qRT-PCR) analysis for TNFAIP1 and NFκB was performed in triplicate with the SYBR Green PCR Master Mix (Perkin-Elmer, Applied Biosystems) according to the manufacturer's instructions. RNA was used to normalize expression. The sequences of the sense and antisense primers were as follows: 5'-GCA CTT TGG CAC CAT TTT GA-3' (F) and 5'-CGG TTC TGA GGG AGG GTG AT-3' (R) for TNFAIP1; 5'-AGGAGAGGATGAAGGAGTTGTG-3' (F) and 5'-CCAGAGTAGCCCAGTTTTTGTC-3 (R) for NFκB. 5'-CCT GTA CGC CAA CAC AGT GC-3' (F) and 5'-ATA CTC CTG CTT GCT GAT CC-3' (R). β-actin data analysis was performed using the $2^{-\Delta\Delta Ct}$ method.

MTT assays. The HeLa and HEC-1A cell lines were seeded in 24-well culture plates, after attachment for 24 h, cells were treated with 25-100 μmol/l caudatin and DMSO as a blank control or transfected with different concentration pCMV-Myc-TNFAIP1 and pCMV-Myc as a blank control. Twenty-four hours later, the cells were incubated with 80 μl MTT at 37˚C for another 4 h. Then the medium was removed and the precipitated formazan was dissolved in 300 μl DMSO. After shaking for 10 min, the absorbance at 420 nm was detected using a microplate spectrophotometer. Three wells were assigned to each group.

Colony formation assay. We detected the effect of caudatin on proliferation in a variety of cultured cell lines (HeLa and HEC-1A). Briefly, 6-well plates were seeded with 500 viable cells, and they were allowed to grow for 24 h. The cells were

treated with 25-100 μmol/l caudatin and DMSO as a blank control. The cells overexpress TNFAIP1 in HEC-1A cells were transfected with different concentration pCMV-Myc-TNFAIP1 and pCMV-Myc-negative as a blank control. The caudatin containing medium was then removed, and the cells were washed in PBS and incubated for an additional 15 days in complete medium. Each treatment was performed in triplicate. The resulting colonies were washed twice with PBS and fixed in methanol for 15 min at room temperature, followed by staining with 20% Giemsa solution for 30 min. The colonies were counted and compared with untreated cells. The colony formation rate was calculated with the following formula. Plate colony formation inhibitory ratio = (number of colonies treated with caudatin/number of cells inoculated) x 100%.

Hoechst 33258 staining. Apoptotic morphological changes in the nuclear chromatin of cells were detected by Hoechst 33258 (Sigma) staining. HeLa and HEC-1A cells were seeded on sterile cover glasses and washed with PBS and fixed with 4% paraformaldehyde for 10 min, and then incubated with 50 μl Hoechst 33258 staining solution for 10 min. After three washes with PBS, the cells were viewed under a fluorescence microscope (Zeiss Axioskop; Zeiss, Oberkochen, Germany).

FACS assays. Cells were harvested at 600 g for 3 min, washed twice in PBS at room temperature and resuspended in appropriate PBS. Then, cells were resuspended in 300 μl 1X FACS banding buffer containing Annexin V and propidium iodide and analyzed using a FACS flow cytometer (BD Biosciences). A total of 10,000 cells were counted for each sample.

Spheroid assay. For formation of spheroids, cell culture was supplemented with 20 ng/ml b-FGF (Invitrogen) 10 ml per 500 ml of 50X B27 supplement (Invitrogen) EGF 20 ng/ml (Invitrogen) and antibiotic and antimycotic solution. HeLa cells were seeded at low densities (5,000 cells/ml) in cell culture bottle. The cells were treated with increasing concentrations of caudatin (0-100 μmol/l). After one week the spheroids were photographed.

Wound-healing assay. HeLa cells and HEC-1A cells were seeded on 6-well plates and grown to 100% confluence. Wounds were created by scraping the monolayer of cells with a sterile pipette tip, washed with PBS to remove the floating cells and incubated with fresh medium in the presence and absence of 25-100 μmol/l caudatin. The images of scratched area were captured using a Leica DMR microscope equipped with DC300F digital camera immediately after wounding and at 24, 48 and 72 h after application of caudatin. The images were compared to estimate the effects of caudatin on wound healing.

Western blot analysis. Treated cells were harvested at the indicated points and lysed in RIPA buffer containing a protease inhibitor and phosphatase inhibitor cocktail. After 3-freeze-thaw cycles in liquid nitrogen, the resulting cell lysates were cleared by centrifugation at 12,000 x g for 10 min at 4˚C, and the proteins were separated by 10% SDS-PAGE. After electrophoresis, the proteins were transferred to polyvinylidene difluorideplus membranes. The membranes were blocked with 50 g/l nonfat milk in TBS washing buffer for 30 min, and then incubated with the indicated primary antibodies at 1:1,000 (Bcl-2, Bax, Cyt-*c*, Caspase-9, Caspase-3, PARP, TNFAIP1, NF-κB, and β-actin) for 3 h or overnight at 4˚C. Then, the membranes were incubated with a 1:2,000 dilution of the proper ALP-conjugated secondary antibody for 1 h at room temperature. After three washes with TTBS (TBS, 0.05% Tween-20), the protein signals were visualized using an ECL Plus kit, according to the manufacturer's instructions. The experiments were repeated at least three times, with protein extracts harvested independently. Densitometry was performed using ImageJ software.

In vivo tumor growth assay. To investigate the tumorigenicity of HeLa cell line, five-week old female BALB/c nude mice were purchased from the SJA Lab Animal (Changsha, China), and allowed to acclimatise for 1 week. The HeLa cells ($1x10^6$) were resuspended in 0.1 ml Dulbecco's modified Eagle's medium and inoculated subcutaneously. Seven days after inoculation, when tumors became palpable, mice were subdivided into two groups of 5 animals each being the tumor volumes equally distributed between the two groups. One group of mice was treated daily with 100 mg/kg caudatin prepared in a solution at mixture of 60% DMSO and 40% alcohol, administered by intraperitoneal injection. The control group received only an injection of same amount of mixture of 60% DMSO and 40% alcohol. The mice were sacrificed and tumors were removed and weighed after the two weeks of caudatin treatment. Primary tumor volumes were calculated with the formula: $v = \text{length} \times (\text{width})^2/2$. All experiments with animals were approved by a local animal committee for ethics.

Statistical analysis. All data are presented as means ± standard deviation from at least three separate experiments. The differences among groups were analyzed using the double-sided Student's t-test, and statistical significance was determined at a P-value of <0.05.

Results

Caudatin reduces viability and clonogenicity of uterine cancer cells. We first quantitatively analyzed the effect of caudatin on cell proliferation in HeLa cells and HEC-1A cells by MTT assay. Treatment with caudatin at the dose of 25-100 μmol/l inhibited cell viability in dose- and time-dependent manner. As shown in Fig. 1A, HeLa cell line viability decreased by 46.06% with 100 μmol/l caudatin after 24 h, and decreased by 50.13% after 36 h. The IC_{50} values for caudatin in HeLa cells at 12, 24, and 36 h were 86.73, 65.85 and 61.60 μmol/l, respectively. HEC-1A cell line viability decrease by 32.1% with 100 μmol/l caudatin after 24 h, and decreased by 50% after 36 h. The IC_{50} values for caudatin in HEC-1A cells at 12, 24 and 36 h were 121.72, 97.49 and 70.70 μmol/l, respectively.

To determine the long-term effect of caudatin treatment, we also tested the effects of caudatin on tumor cell clonogenicity in HeLa and HEC-1A cells (Fig. 1B). Cells were treated with different concentrations of caudatin for 24 h, and then the cells were allowed to grow in normal media. Treatment with caudatin markedly inhibited colony formation, resulting in a decrease by 70.24% with 100 μmol/l caudatin after 24 h

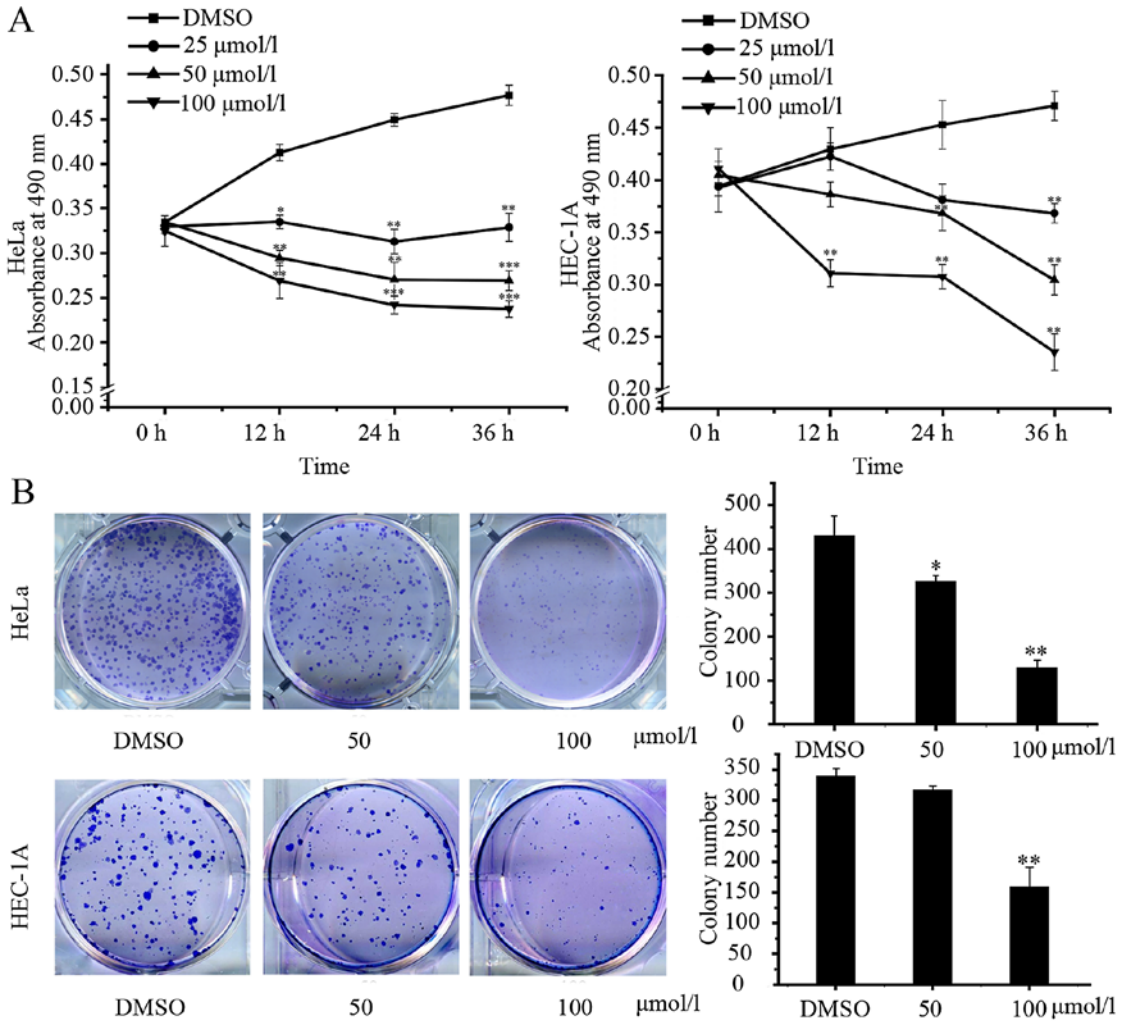

Figure 1. Caudatin suppresses uterine cancer cell line proliferation and colony formation. (A) HeLa and HEC-1A cells were treated with caudatin at the indicated doses. The cell viability was determined by a MTT assay. Caudatin treatment resulted in a significant dose- and time-dependent decrease in cell proliferation in the two cell lines when compared with the untreated controls (*P<0.05; **P<0.01; ***P<0.001). (B) Cell viability was determined using colony formation assays. Uterine cancer cells were left overnight to attach before addition of indicated doses of caudatin for 24 h. The plates were left for 15 days without change of medium, and then cells were harvested and treated with Giemsa stain, and counted. Incubation with caudatin inhibits colony formation. The data are presented as mean ± SD of three tests. Data are expressed as mean ± SEM, *P<0.05, **P<0.01.

at HeLa and decrease by 54.24% with 100 μmol/l caudatin after 24 h at HEC-1A cells. Notably, the HeLa cells presented a higher sensitivity than the HEC-1A cells. These results indicate that caudatin inhibits the growth of HeLa and HEC-1A cells in a dose- and time-dependent manner.

Caudatin treatment induces apoptosis in HeLa and HEC-1A cells. The induction of apoptosis is considered as one of the possible mechanisms of inhibition of cancer development. Caudatin is known to induce apoptosis in variety of cancer cells, which is considered to be an important mechanism for their antitumor activity and prevention of carcinogenesis (13,14). Annexin V-FITC/PI double-labeled flow cytometry was used to assess the ratio of apoptotic HeLa cells following caudatin treatment. The total apoptosis ratio was the sum of the early apoptotic and late apoptotic ratios. The apoptosis rates for HeLa cells treated with different concentrations (25,50 and 100 μmol/l) of caudatin for 24 h were 6.23±0.48, 8.68±1.89% and 14.83±1.43%, respectively, which were significantly higher than that of the control group (4.04±0.62%) (as shown in Fig. 2A). Moreover, Hoechst 33258 staining revealed typical morphological changes, such as the formation of apoptotic bodies, after 24-h treatment with different concentrations (25-100 μmol/l) of caudatin, whereas the control cells did not show apoptosis-related morphological changes (Fig. 2B). Normal nuclei were identified as having non-condensed chromatin dispersed over the entire nucleus, and apoptotic nuclei were identified as having condensed chromatin that was contiguous with the nuclear membrane and/or fragmented nuclei. Overall, these results are consistent with cell apoptosis by Hoechst 33258 staining and flow cytometry analysis, suggesting that the inhibition of cell growth by caudatin may be associated with induction of apoptosis.

Caudatin-induced apoptosis is mediated via caspase activation in uterine cancer cell lines. To confirm the effect of caudatin on apoptosis, we next detected the expression of some pro-apoptotic and antiapoptotic proteins, cytochrome *c* (Cyt *c*), BAX, Bcl-2 caspase-3/9 and PARP in HeLa and HEC-1A cells by western blot analysis. Caudatin markedly increased

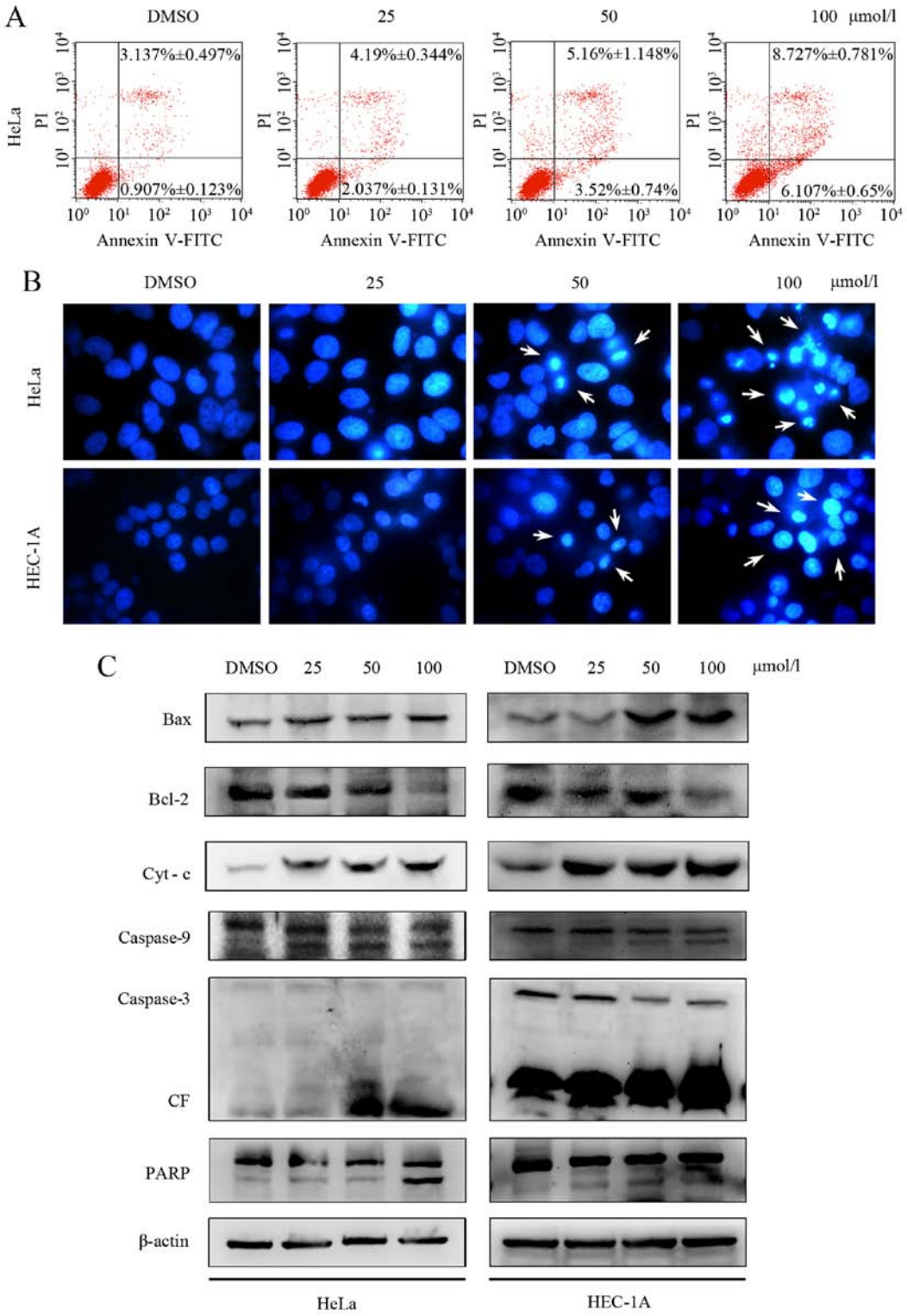

Figure 2. Caudatin changes cell morphology and activates the apoptotic pathway in uterine cancer cell lines. (A) HeLa cells were treated with different concentrations of caudatin for 24 h, and then analyzed for apoptosis by flow cytometry for Annexin V and PI staining. Numbers in the respective quadrant profiles indicate the percentage of apoptotic cells. (B) Morphology of apoptotic cell nuclei was observed by Hoechst staining using a fluorescence microscope (magnification, x40). The control group was treated with DMSO. (C) Western blot analyses showed a reduction of cytochrome *c* and the cleavage of caspase-9, -8, -3, and PARP in response to various concentrations of caudatin. Caudatin reduced the expression of the anti-apoptotic protein, Bcl-2, whereas it increased the expression of pro-apoptotic protein Bax compared to untreated cells. β-actin was used as a control. One representative of three different experiments is shown.

the expression levels of Bax protein, but decreased the Bcl-2 protein levels, as compared with the control group. The release of Cyt-*c* from the mitochondrial inter-membrane space into the cytosol is the precondition of caspase-dependent apoptosis pathway. The expression level of full-length caspase-9 and -3 was decreased, suggesting cleavage and activation of

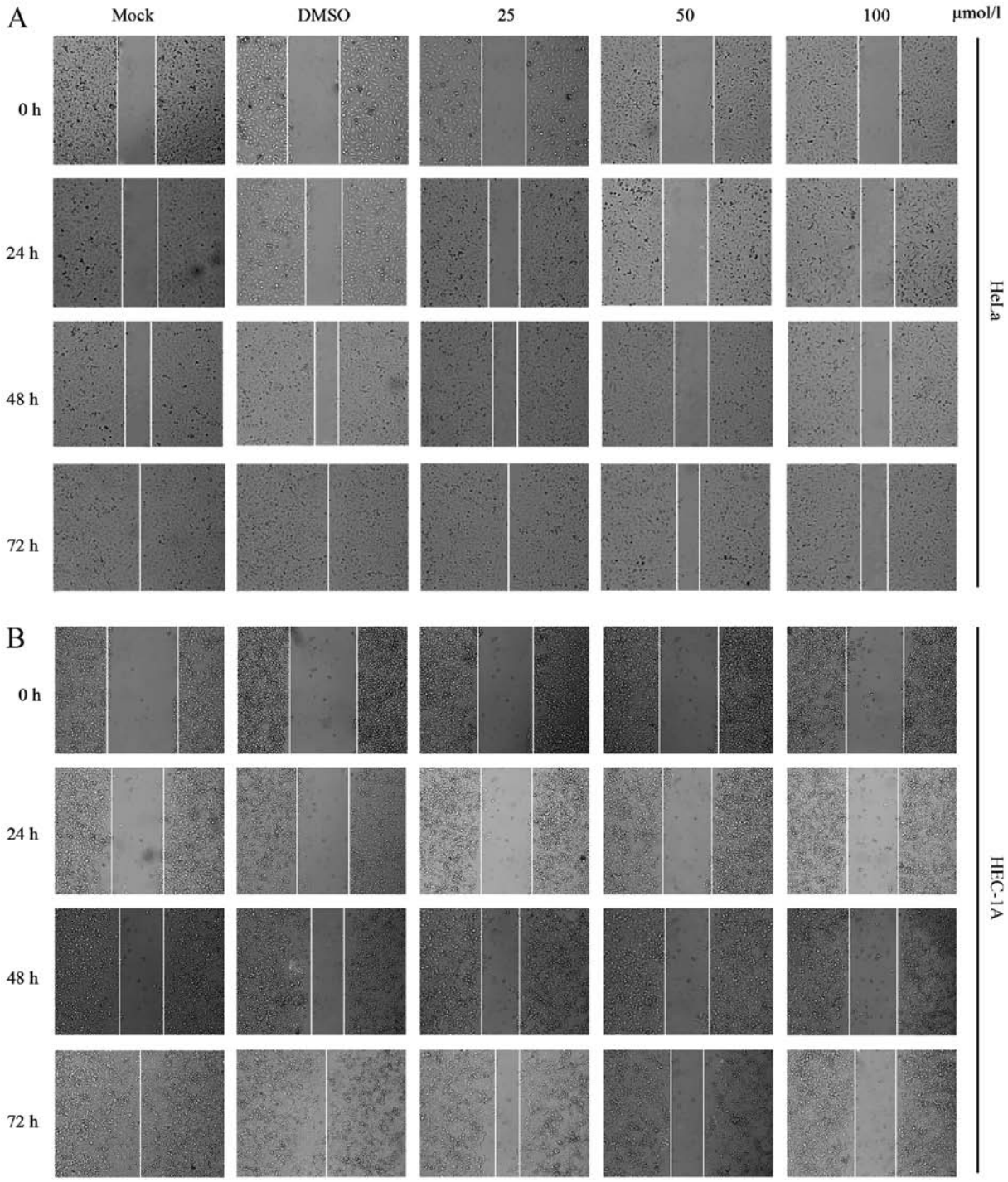

Figure 3. Cell migration was analyzed by a wound-healing assay. Cells of HeLa (A) and HEC-1A (B) grown in monolayer were scratched with a pipette tip and then treated with different concentrations of caudatin. Cell motility was assessed by light microscopy and micrographs were taken at 0, 24, 48 and 72 h, respectively.

the caspase pathway. Furthermore, PARP, which is the prime marker for caspase-dependent apoptosis, showed cleavage in a dose-dependent manner (Fig. 2C). These data demonstrate that caudatin is a potent inducer of apoptosis in cervical carcinoma and endometrial carcinoma cells, and the apoptosis involves the caspase-related pathway.

Caudatin inhibited cell migration. We also tested the effect of caudatin on cell migration by employing a wound-healing assay. As shown in Fig. 3A, the part of the wounding space between cell layers after making a scratch was occupied completely by the migrating cells after 72 h in the control group and the group treated with 25 μmol/l caudatin in the HeLa cell line. However, the empty space of the cells was not occupied by the migrating cells treated with 50 or 100 μmol/l caudatin. Similar result of HEC-1A cell line is shown in Fig. 3B. These results demonstrate the potential of caudatin in inhibiting cell migration in uterine tumor cells.

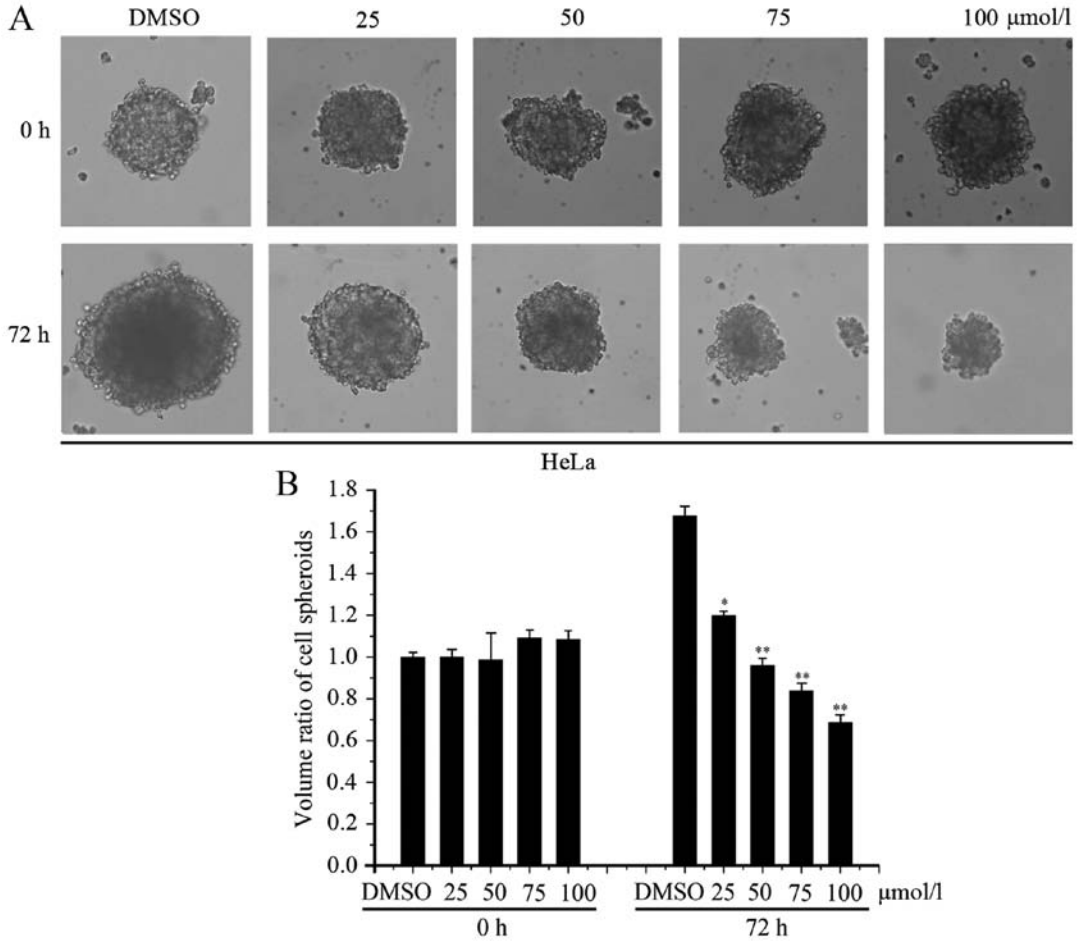

Figure 4. Caudatin inhibites spheroid formation. (A) HeLa cells were grown in low adherent plates and treated with increasing concentrations of caudatin (0, 25, 50 and 100 μmol/l) for the spheroid assay. After 72 h the spheroids were photographed. (B) Caudatin treatment significantly inhibited cervical carcinoma cell spheroids. The volume ratio of cell spheroid was counted and shown as the bar diagram (*P<0.05; **P<0.01).

Caudatin inhibits spheroid formation of HeLa cells. The 3-D cellular model should be used to better mimic the *in vivo* environments (e.g., diffusion and transport conditions of drugs, nutrients, and oxygen). Formation of cell spheroids is one of the essential tools for studying the behaviors of a 3-D cellular model. Cell spheroids are also more reliable material than two-dimensional (2-D) cellular models for drug screening in clinical research (30,31). We next determined the effects of caudatin on cervical carcinoma cell spheroid formation. As shown in Fig. 4A, caudatin treatment significantly inhibited cell sphere formation in a dose-dependent manner in HeLa cells. The spheroids size was counted (Fig. 4B). These results demonstrated caudatin treatment reduced spheroid formation.

TNFAIP1 is downregulated in human uterine carcinoma tissues. The correlation of TNFAIP1 expression with various clinicopathologic factors was analyzed. To confirm the expression level of TNFAIP1 in uterine cancer tissues and normal uterine tissues, total RNA was extracted from 16 uterine cancer samples, consisting of four stage I of moderate differentiation, seven stage I-II of moderate differentiation and six stage I-II of poorly differentiation uterine cancer tissues, 16 matched normal tissues, and then quantitative real-time PCR was performed to analyze the expression profile. As shown in Fig. 5, we found that TNFAIP1 had lower expression levels in the 12 uterine cancer tissues (UC; 5-11, stage I-II of moderate differentiation; and 12-16, stage I-II of poor differentiation) when compared with that in the paired adjacent non-tumorous tissues (N), and 4 tissues had higher expression (UC; 1-4, stage I of moderate differentiation). This study has shown the expression of TNFAIP1 in uterine cancer tissues to be consistent with a previous study in cancer cell lines, indicating a possible role as an antioncogene.

Caudatin regulates the expression of NFκB (p65) through TNFAIP1. NF-κB has been regarded as the hallmark of carcinogenesis and the expression of NF-κB is tightly controlled by TNFAIP1. In this study, we found that TNFAIP1 is expressed at low level in HeLa and HEC-1A cell lines. After pCMV-Myc-TNFAIP1 was transfected into the uterine cancer cells for 24 h, the expression levels of TNFAIP1 protein levels of TNFAIP1 and p65NF-κB were detected by western blotting, indicating increased expression of TNFAIP1 and decreased expression of p65NF-κB in the overexpression TNFAIP1 group compared with the NC and MOCK groups (Fig. 6A). The expression level of p65NF-κB protein was found to be significantly downregulated in the pCMV-Myc-TNFAIP1 group when compared with the level in the NC and NC

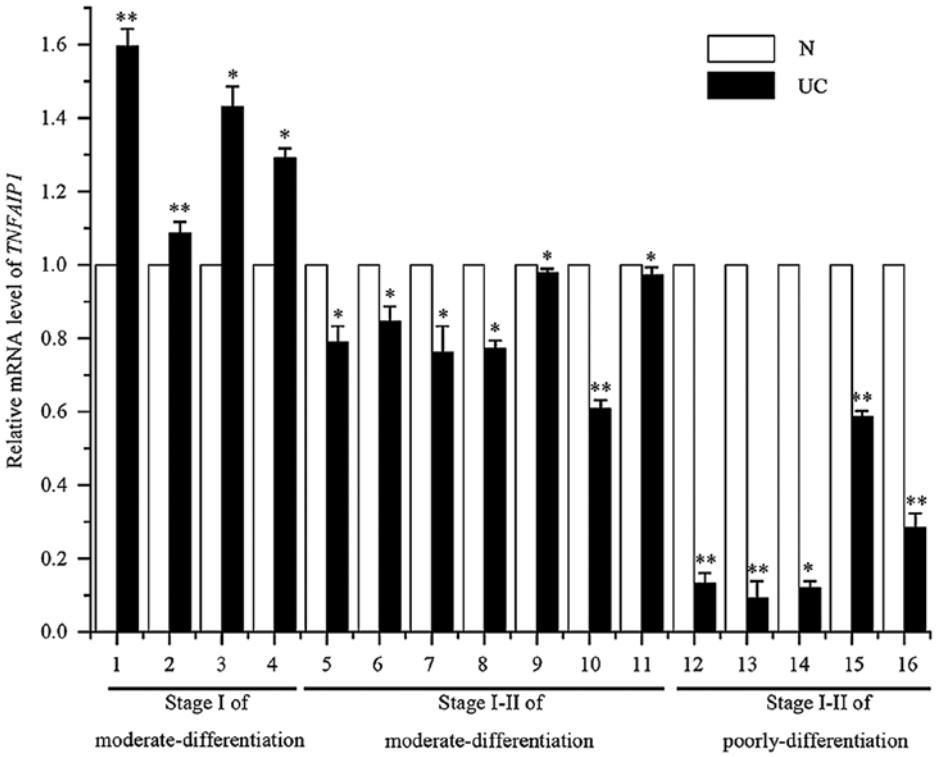

Figure 5. TNFAIP1 is downregulated in human uterine cancer tissues compared to normal uterine tissues. QRT-PCR analysis of TNFAIP1 in 16 pairs of uterine adenocarcinoma tissues (Uc; 1-4, stage I of moderate differentiation; 5-11, stage I-II of moderate differentiation; 12-16, stage I-II of poor differentiation and matched adjacent normal tissues (N). The data represent the mean ± SD of three different experiments. *P<0.05 or **P<0.01 vs. adjacent normal tissues.

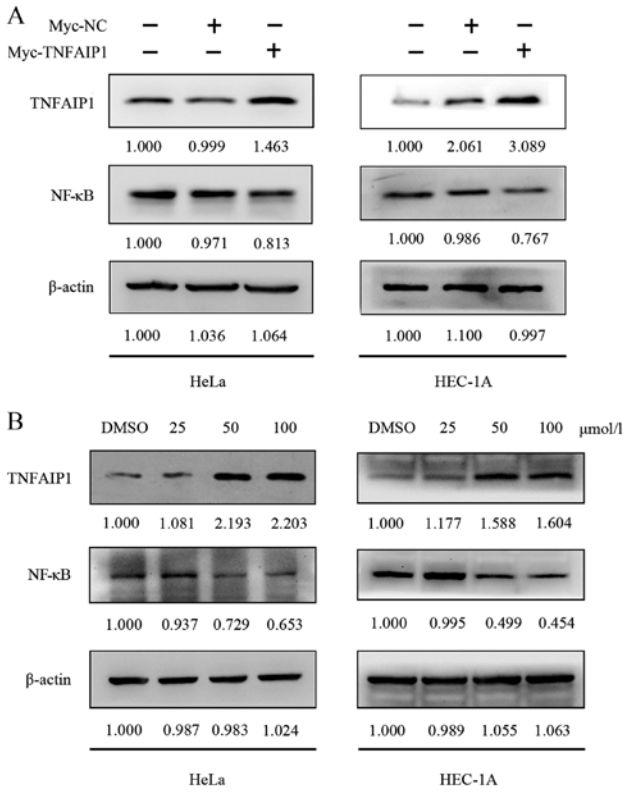

Figure 6. Caudatin regulates the expression of NF-κB (p65) through TNFAIP1. (A) While TNFAIP1 was overexpressed in HeLa and HEC-1A cells, NF-κB presented downregulation accompanied by increased TNFAIP1. (B) TNFAIP1 and NF-κB expression were determined by western blot analysis after treatment with caudatin in HeLa and HEC-1A cells. One representative of three different experiments is shown. Images were converted to gray scale and analyzed using ImageJ software.

groups. To determine whether caudatin targets the TNFAIP1/NF-κB signaling, we treated HeLa and HEC-1A cells with caudatin (25, 50 or 100 μmol/l) and examined the expression of TNFAIP1 and NF-κB proteins by western blotting, respectively. These results demonstrate that caudatin upregulated expression of TNFAIP1 in a dose-dependent manner. Along with TNFAIP1 expression improved by induction of caudatin in the HeLa and HEC-1A cells, NF-κB showed downregulation (Fig. 6B). TNFAIP1 regulated by caudatin may finally have an effect on NF-κB signaling. Consequently, caudatin that can regulate the expression of TNFAIP1 could potentially have therapeutic value.

The effect of TNFAIP1 overexpression is consistent with caudatin treated in HEC-1A cells. To confirm the effect of TNFAIP1 on uterine cancer growth, we examined cell proliferative activities by MTT assay and colony formation. The results showed that overexpression of TNFAIP1 suppressed the proliferative activities of the uterine cancer cells in a time- and dose-dependent manner compared to the NC group (Fig. 7A) and inhibited colony formation (Fig. 7B). Moreover, Hoechst 33258 staining indicated that typical apoptotic cell morphology, such as the formation of apoptotic bodies, appeared after cells were transfected with TNFAIP1, while the control cells did not show evident apoptotic morphological changes (Fig. 7C). In brief, these results demonstrated that TNFAIP1 produces the same effect as caudatin treatment in uterine cancer cells and indicated that caudatin regulate cell growth, apoptosis of uterine cancer cells by targeting TNFAIP1.

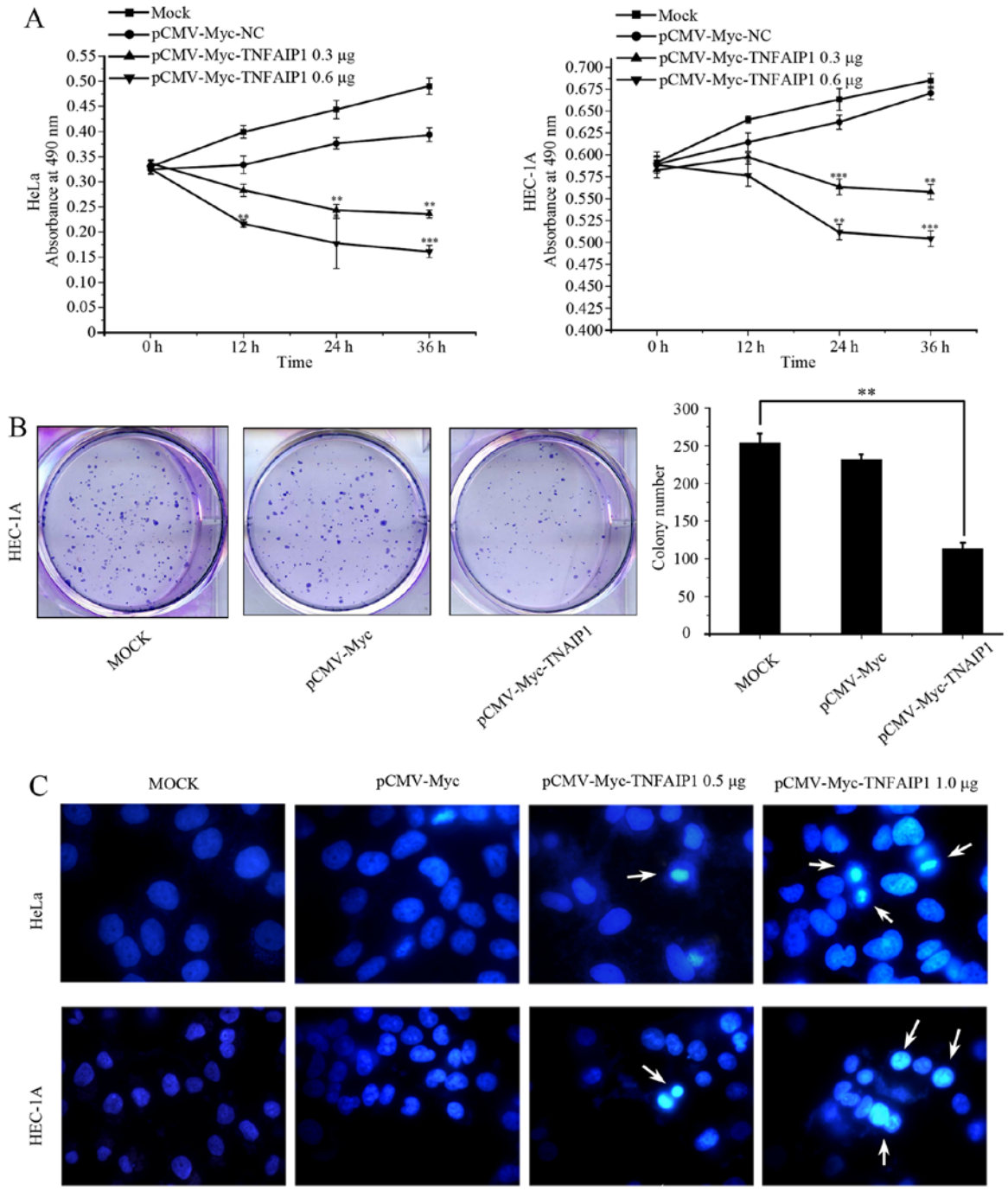

Figure 7. Cell viability is inhibited and cell apoptosis is induced by pCMV-Myc-TNFAIP1. (A) MTT assay was used to examine the effect of overexpression of TNFAIP1 in proliferation of HeLa cells and HEC-1A cells. (B) Cell viability was determined using colony formation assays. (C) Hoechst staining revealed HeLa cells and HEC-1A cell apoptosis compared to mock and with pCMV-TNFAIP1 or pCMV empty vector. Data are expressed as mean ± SEM, ***P<0.005, **P<0.01.

Caudatin inhibits tumorigenicity in vivo. We then tested the caudatin inhibition of tumorigenicity *in vivo*. HeLa cells ($1x10^6$) were resuspended in 0.1 ml Dulbecco's modified Eagle's medium and inoculated subcutaneously. Seven days after inoculation, when tumors became palpable, mice were subdivided into two groups of 5 animals each in which the tumor volumes were equally distributed between the groups. One group of mice was treated daily with 100 mg/kg caudatin. In the experiment presented, the animal was treated with the drugs for a period of 14 days. Compared to the vehicle (60% DMSO and 40% alcohol), caudatin significantly decreased tumor size, overall tumor weight, and mean tumor volume in 2 weeks after injection. In order to verify the results, we repeated the experiment. The general conditions and the body weight of the animals treated with caudatin showed nearly no change for the period of caudatin application, which implies that the compound has no obvious toxicity to experiment animals (Fig. 8A and B). These results indicate caudatin has potential as a novel tumor suppressor that can suppress tumor growth.

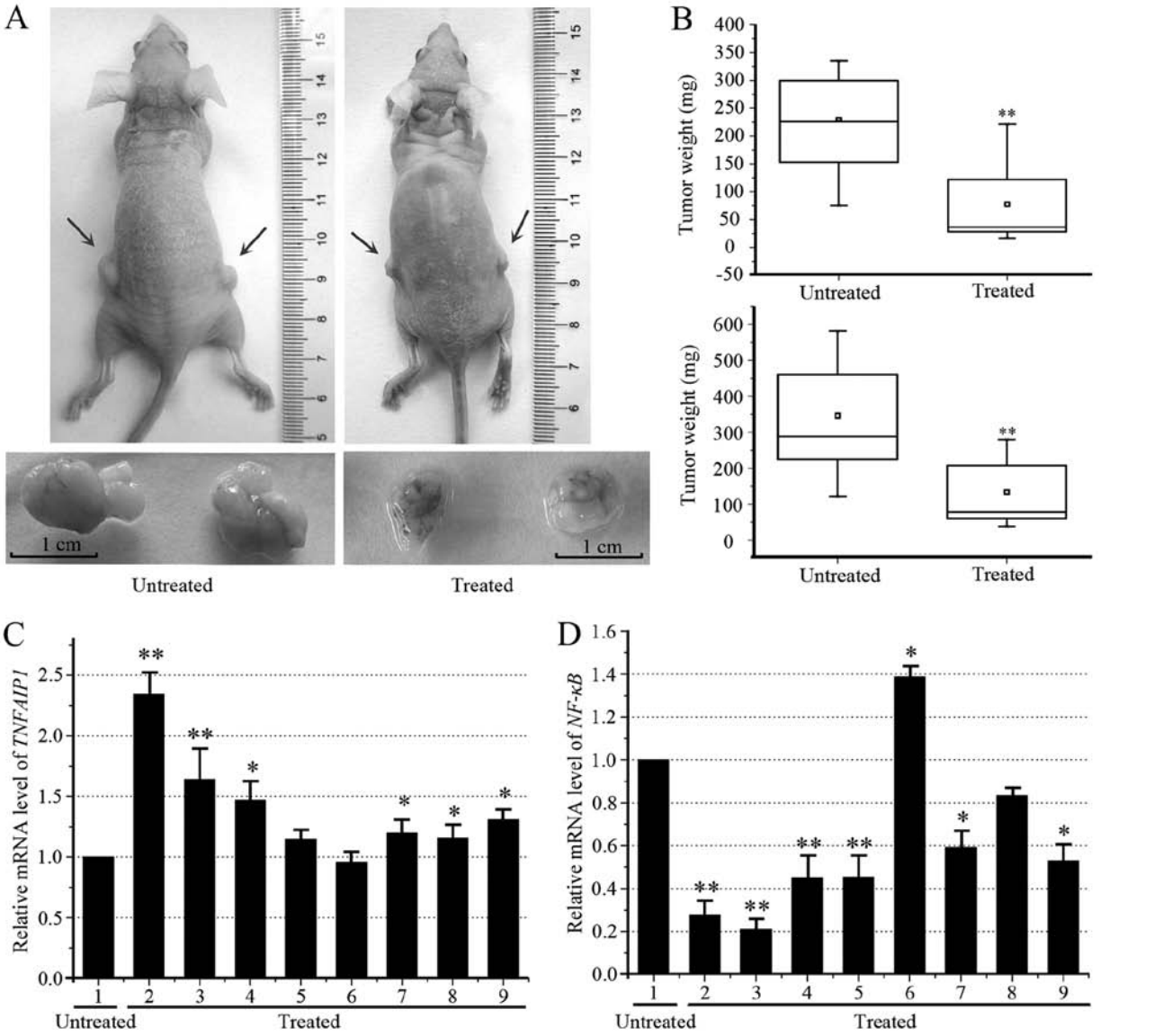

Figure 8. Caudatin inhibits tumorigenicity *in vivo*. (A) The effect of caudatin on tumor growth. After 7 days of tumor establishment, mice were treated by intraperitoneal injection with caudatin 100 mg/kg/daily. Progression profile of tumor growth was compared with that of control mice treated with DMSO alone. (B) The weight and volume of the treated tumors were decreased. (C and D) qRT-PCR assay indicates that caudatin increased the mRNA level of TNFAIP1 and downregulated the mRNA level of NF-κB. Data are expressed as mean ± SEM, *P<0.05, **P<0.01.

We also observed a significant inverse correlation between TNFAIP1 and NF-κB by treatment with caudatin. In the two tests, the tumours of two mice were small in the treated group and therefore total RNA extraction could not be performed, our qRT-PCR assay indicates that caudatin increased the mRNA level of TNFAIP1 (Fig. 8C) and downregulated the mRNA level of NF-κB (Fig. 8D) in the other tumours of eight mice.

Discussion

Uterine cancer is a common type of cancer among women, and its incidence is increasing worldwide. Tumor metastasis poses a predominant threat to cancer-related mortality (34). Despite uterine tumor being frequently diagnosed cancer and the recent advances in the treatment of uterine tumor, there are patients for whom no targeted therapies are available. The significant morbidity, toxicity and poor response rates of current chemotherapy regimens have led to search for less toxic alternative therapies (35). It was previously reported that caudatin suppresses proliferation and induces apoptosis in a variety of tumor cells; however, the molecular mechanisms underlying these effects are still unclear.

MTT assay was performed to quantify the effects of caudatin on HeLa and HEC-1A cell growth inhibition. The data presented here showed that caudatin treatment resulted in a dose- and time-dependent inhibition of proliferation in HeLa and HEC-1A cells. The IC_{50} values for caudatin in HeLa cells at 12, 24, and 36 h were 86.73, 65.85 and 61.60 μmol/l, respectively. The IC_{50} values for caudatin in HEC-1A cells at 12, 24, and 36 h were 121.72, 97.49 and 70.70 μmol/l, respectively. Moreover, caudatin treatment suppressed colony formation in HeLa and HEC-1A cells tested, suggesting that the caudatin effect on the tumor cells is irreversible. In addi-

tion to inappropriate growth signals, many cancer cells lose their ability to undergo apoptosis. Disturbances in apoptosis are important for the development of cancer (36). Therefore, the killing of tumors through induction of apoptosis has been recognized as a novel strategy for the identification of anticancer drugs (37). In order to distinguish that the cell death caused by caudatin is due to apoptosis or necrosis, Annexin V/PI double-labeling analysis was performed which enables further distinction of necrotic/late apoptotic (Annexin V^+/PI^+) and early apoptotic (Annexin V^+/PI^-) cells. Our results showed that treatment of HeLa cells with caudatin resulted in a dose-dependent increase in the numbers of both early apoptotic and late apoptotic/necrotic cells. The treatment of HeLa cells with various concentrations of caudatin (25, 50 and 100 μmol/l) resulted in apoptosis rates of 4.19±0.344, 5.16±1.15 and 8.73±0.78%, respectively, which were significantly higher than that of the control group (3.14±0.50%). Indeed, we observed a significant increase in dead cells in the HeLa cells even at 12 h following incubation with caudatin, which subsequently led to cell death. Hoechst staining showed that the typical morphological changes attributed to apoptosis, such as formation of apoptotic bodies, appeared after the cells were treated for 24 h with 25-100 μmol/l caudatin, whereas the control cells did not show evident apoptotic morphological changes. Caspases, a family of cysteine proteases, are synthesized as inactive pro-enzymes which are processed to an active form in cells undergoing apoptosis (38,39). In this study, we demonstrated that caudatin treatment triggered cytochrome *c* release from mitochondrial inter-membrane space into cytosol, affected expression of BAX and Bcl-2, and promoted cleavage of caspase-3, -9 and PARP, thereby activating apoptotic pathway. Thus, the induction of HeLa and HEC-1A cell apoptosis in response to caudatin is an important mechanism for its preventative and antitumor activity in uterine cancer.

Wound-healing assay was a mature approach to test cell migration ability. Our experimental results suggested that caudatin markedly reduced the migration ability of cells compared to scramble group cells. As shown in Fig. 3, the part of the wounding space between cell layers after making a scratch was occupied completely by the migrating cells after 72 h in the control group. However, the empty space of the cells was not occupied by the migrating cells treated with 50 and 100 μmol/l caudatin. These results demonstrated the potential of caudatin in changing cell morphology and inhibiting cell migration in uterine cancer cells. Cancer cells possess varying capacities for spheroid formation and although a positive correlation with tumorigenicity has been suggested (40,41), another study reported an inverse association between brain tumor cell spheroid cohesiveness and invasive potential (42). Although spheroid formation affords protection of cancer cells against some chemotherapeutic agents, it has not been established whether a relationship exists between invasive behavior and predisposition to spheroid formation. The cell behavior necessary for compact spheroid formation may also promote uterine cancer progression (43). In this study, HeLa cells were grown in low adherent plates and treated with increasing concentrations of caudatin (0-100 μmol/l) and performed in the spheroid assay. Caudatin treatment significantly inhibited uterine cancer cells spheroids. The results revealed caudatin play a potential suppressive role and antitumor activity in uterine cancer.

Advances in the understanding of the molecular mechanisms of apoptosis have identified the apoptotic pathway as a promising target to increase the effectiveness of cancer treatment. It has been previously reported that TNFAIP1 was shown to be expressed at a high level in normal cells and was downregulated in several cancer derived cell lines. In tumor cells, TNFAIP1 can act through pleiotropic mechanisms, including stimulation of cell proliferation, survival, migration, and invasion (24,27). Initially found to be an anti-oncogene in metastatic breast cancer (44). NF-κB is one of the most important intracellular nuclear transcription factors, and it plays a central role in the transcriptional regulation of many genes that are influenced by various stimuli. It has also been shown that NF-κB activity inhibits apoptosis in cancer cells. In a previous study, we found that TNFAIP1 and KCTD10 suppressed the transcriptional activities of NF-κB, leading to discreased cell survival by transactivating anti-apoptotic genes downstream of NF-κB (29,45). A recent study indicated that high expression of TNFAIP1 was associated with distant metastasis of osteosarcoma, and knockdown of TNFAIP1 inhibited the growth and invasion, and induced apoptosis in osteosarcoma cells through inhibition of the NF-κB pathway, suggesting that TNFAIP1 may act as a potential therapeutic target for the treatment of cancer (25,26). Whereas TNFAIP1 upregulation inhibited tumor growth, suggesting that TNFAIP1 might play a key role in maintaining cancer cell survival. In this study, we found that TNFAIP1 is frequently downregulated in uterine cancer tissues (Fig. 5). We found that while pCMV-Myc-TNFAIP1 was transfected to HeLa or HEC1A cells, NF-κB presented downregulation accompanied by increased TNFAIP1. Moreover, the overexpression of TNFAIP1 could inhibit cell proliferation, colony formation, and induces apoptosis in HEC-1A cells similarly to those induced by caudatin. Therefore, we hypothesized that caudatin exerts its effects through the modulation of the expression of TNFAIP1. As shown in Fig. 6B, experimental confirmation demonstrated that TNFAIP1 gene is a potential target of caudatin and can be regulated by caudatin in a dose-dependent manner. Moreover, we found that caudatin treatment led to an ~50% increasion in TNFAIP1 and an ~40% reduction in NF-κB protein levels. Collectively, our data indicate that tumor suppression function of caudatin may be through control of cell growth, migration and cell apoptosis by upregulating the TNFAIP1 and negatively regulating NF-κB expression.

To further explore the role of caudatin in tumor growth *in vivo*, HeLa cells ($1x10^6$) were injected subcutaneously into nude mice. Seven days after inoculation, when tumors became palpable, mice were subdivided into two groups of 5 animals each with the tumor volumes equally distributed between the two groups. One group of mice was injected daily with 100 mg/kg caudatin. Compared to the vehicle (DMSO), caudatin significantly decreased tumor size, overall tumor weight, and mean tumor volume in 2 weeks after injection. Treatment with caudatin induced smaller tumors than the control *in vivo* and their average volume was 36.9% of the control group at day 14 after injection ($P<0.05$) (Fig. 8B). As expected, the expression of TNFAIP1 was increased in

xenograft animal tumors treated with caudatin (Fig. 8C). However, the expression of NF-κB was significantly suppressed in caudatin-treated tumors (Fig. 8D). These results indicated that caudatin might function as a tumor suppressor drug partly mediated by repressing TNFAIP1 expression in uterine cancer. However, TNFAIP1 is not the only pathway inhibited in uterine cancer, as many other signal transduction pathways are inhibited, and these pathways will be the focus of our future research.

In conclusion, we demonstrated that caudatin exhibited anti-proliferative and pro-apoptotic activities in uterine cancer cells, at least partially, via the caspase-dependent apoptotic pathway and the TNFAIP1/NF-κB signaling pathway. Thus, targeting TNFAIP1 may be an effective strategy to control tissue destruction in uterine cancer patients. Our findings provide new insights into exploring the potential therapeutic strategies and novel targets for human uterine cancer.

Acknowledgements

This study was supported by the National Natural Science Foundation of China (grant nos. 81071696 and 81372157), Project of Inquiry Learning and Innovative Experiment of Hunan Province (2014-075), Project of Innovative Experiment of Hunan Normal University (043-0094), The Cooperative Innovation Center of Engineering and New Products for Developmental Biology of Hunan Province (20134486), and the Construct Program of the Key Discipline of Basic Medicine in Hunan Province in China.

References

1. Ferlay J, Shin HR, Bray F, Forman D, Mathers C and Parkin DM: Estimates of worldwide burden of cancer in 2008: GLOBOCAN 2008. Int J Cancer 127: 2893-2917, 2010.
2. Barbera L and Thomas G: Management of early and locally advanced cervical cancer. Semin Oncol 36: 155-169, 2009.
3. Yang Y, Li Y, Li J, Wang J and Yan Z: Tendency and strategy of younger patients with cervical carcinoma. Med Natl Defending Forces Southwest China 1: 53-55, 2008.
4. Huang CY, Chen CA, Chen YL, Chiang CJ, Hsu TH, Lin MC, Lai MS, Chen CJ, You SL and Cheng WF: Nationwide surveillance in uterine cancer: survival analysis and the importance of birth cohort: 30-year population-based registry in Taiwan. PLoS One 7: e51372, 2012.
5. Zhang Z, Li B, Meng X, Yao S, Jin L, Yang J, Wang J, Zhang H, Zhang Z, Cai D, *et al*: Berberine prevents progression from hepatic steatosis to steatohepatitis and fibrosis by reducing endoplasmic reticulum stress. Sci Rep: Feb 9, 2016 (Epub ahead of print). doi: 10.1038/srep20848.
6. Yu D, An F, He X and Cao X: Curcumin inhibits the proliferation and invasion of human osteosarcoma cell line MG-63 by regulating miR-138. Int J Clin Exp Pathol 8: 14946-14952, 2015.
7. Tian L, Shen D, Li X, Shan X, Wang X, Yan Q and Liu J: Ginsenoside Rg3 inhibits epithelial-mesenchymal transition (EMT) and invasion of lung cancer by down-regulating FUT4. Oncotarget 7: 1619-1632, 2016.
8. Vistad I, Fosså SD and Dahl AA: A critical review of patient-rated quality of life studies of long-term survivors of cervical cancer. Gynecol Oncol 102: 563-572, 2006.
9. Ma XX, Wang D, Zhang YJ and Yang CR: Identification of new qingyangshengenin and caudatin glycosides from the roots of *Cynanchum otophyllum*. Steroids 76: 1003-1009, 2011.
10. Yin ZQ, Yu SL, Wei YJ, Ma L, Wu ZF, Wang L, Zhang QW, Zhao M, Ye WC, Che CT, *et al*: C21 steroidal glycosides from Cynanchum Stauntonii induce apoptosis in HepG2 cells. Steroids 106: 55-61, 2016.
11. Wang YQ, Zhang SJ, Lu H, Yang B, Ye LF and Zhang RS: A C_{21}-steroidal glycoside isolated from the roots of *cynanchum auriculatum* induces cell cycle arrest and apoptosis in human gastric cancer SGC-7901 cells. Evid Based Complement Alternat Med 2013: 180839, 2013.
12. Fu XY, Zhang S, Wang K, Yang MF, Fan CD and Sun BL: Caudatin inhibits human glioma cells growth through triggering DNA damage-mediated cell cycle arrest. Cell Mol Neurobiol 35: 953-959, 2015.
13. Fei HR, Cui LY, Zhang ZR, Zhao Y and Wang FZ: Caudatin inhibits carcinomic human alveolar basal epithelial cell growth and angiogenesis through modulating GSK3β/β-catenin pathway. J Cell Biochem 113: 3403-3410, 2012.
14. Li X, Zhang X, Liu X, Tan Z, Yang C, Ding X, Hu X, Zhou J, Xiang S, Zhou C, *et al*: Caudatin induces cell apoptosis in gastric cancer cells through modulation of Wnt/β-catenin signaling. Oncol Rep 30: 677-684, 2013.
15. Peng Y and Ding Y: Pharmacokinetics and tissue distribution study of caudatin in normal and diethylnitrosamine-induced hepatocellular carcinoma model rats. Molecules 20: 4225-4237, 2015.
16. Luo Y, Sun Z, Li Y, Cai X and Li Z: Caudatin inhibits human hepatoma cell growth and metastasis through modulation of the Wnt/β-catenin pathway. Oncol Rep 30: 2923-2928, 2013.
17. Wang LJ, Geng CA, Ma YB, Luo J, Huang XY, Chen H, Zhou NJ, Zhang XM and Chen JJ: Design, synthesis, and molecular hybrids of caudatin and cinnamic acids as novel anti-hepatitis B virus agents. Eur J Med Chem 54: 352-365, 2012.
18. Peng YR, Ding YF, Wei YJ, Shu B, Li YB and Liu XD: Caudatin-2,6-dideoxy-3-O-methy-β-D-cymaropyranoside 1 induced apoptosis through caspase 3-dependent pathway in human hepatoma cell line SMMC7721. Phytother Res 25: 631-637, 2011.
19. Wolf FW, Marks RM, Sarma V, Byers MG, Katz RW, Shows TB and Dixit VM: Characterization of a novel tumor necrosis factor-alpha-induced endothelial primary response gene. J Biol Chem 267: 1317-1326, 1992.
20. Link CD, Taft A, Kapulkin V, Duke K, Kim S, Fei Q, Wood DE and Sahagan BG: Gene expression analysis in a transgenic Caenorhabditis elegans Alzheimer's disease model. Neurobiol Aging 24: 397-413, 2003.
21. Yang L, Liu N, Hu X, Zhang W, Wang T, Li H, Zhang B, Xiang S, Zhou J and Zhang J: CK2 phosphorylates TNFAIP1 to affect its subcellular localization and interaction with PCNA. Mol Biol Rep 37: 2967-2973, 2010.
22. Zhou C, Li X, Zhang X, Liu X, Tan Z, Yang C and Zhang J: microRNA-372 maintains oncogene characteristics by targeting TNFAIP1 and affects NFκB signaling in human gastric carcinoma cells. Int J Oncol 42: 635-642, 2013.
23. Zhang X, Li X, Tan Z, Liu X, Yang C, Ding X, Hu X, Zhou J, Xiang S, Zhou C, *et al*: MicroRNA-373 is upregulated and targets TNFAIP1 in human gastric cancer, contributing to tumorigenesis. Oncol Lett 6: 1427-1434, 2013.
24. Zhu Y, Yao Z, Wu Z, Mei Y and Wu M: Role of tumor necrosis factor alpha-induced protein 1 in paclitaxel resistance. Oncogene 33: 3246-3255, 2014.
25. Tian X, Zhang J, Yan L, Dong JM and Guo Q: miRNA-15a inhibits proliferation, migration and invasion by targeting TNFAIP1 in human osteosarcoma cells. Int J Clin Exp Pathol 8: 6442-6449, 2015.
26. Zhang CL, Wang C, Yan WJ, Gao R, Li YH and Zhou XH: Knockdown of TNFAIP1 inhibits growth and induces apoptosis in osteosarcoma cells through inhibition of the nuclear factor-κB pathway. Oncol Rep 32: 1149-1155, 2014.
27. Yang LP, Zhou AD, Li H, Zhang WF, Wu YY, Zhang J and Han M: Expression profile in the cell lines of human TNFAIP1 gene. Yi Chuan 28: 918-922, 2006 (In Chinese).
28. Kim DM1, Chung KS, Choi SJ, Jung YJ, Park SK, Han GH, Ha JS, Song KB, Choi NS, Kim HM, *et al*: RhoB induces apoptosis via direct interaction with TNFAIP1 in HeLa cells. Int J Cancer 125: 2520-2527, 2009.
29. Hu X, Yan F, Wang F, Yang Z, Xiao L, Li L, Xiang S, Zhou J, Ding X and Zhang J: TNFAIP1 interacts with KCTD10 to promote the degradation of KCTD10 proteins and inhibit the transcriptional activities of NF-κB and AP-1. Mol Biol Rep 39: 9911-9919, 2012.
30. Lin RZ and Chang HY: Recent advances in three-dimensional multicellular spheroid culture for biomedical research. Biotechnol J 3: 1172-1184, 2008.

31. Patra B, Peng CC, Liao WH, Lee CH and Tung YC: Drug testing and flow cytometry analysis on a large number of uniform sized tumor spheroids using a microfluidic device. Sci Rep: Feb 15, 2016 (Epub ahead of print). doi: 10.1038/srep21061.
32. Daniyal M, Akhtar N, Ahmad S, Fatima U, Akram M and Asif HM: Update knowledge on cervical cancer incidence and prevalence in Asia. Asian Pac J Cancer Prev 16: 3617-3620, 2015.
33. Singh R: Review literature on uterine carcinosarcoma. J Cancer Res Ther 10: 461-468, 2014.
34. Jemal A, Siegel R, Ward E, Hao Y, Xu J, Murray T and Thun MJ: Cancer statistics, 2008. CA Cancer J Clin 58: 71-96, 2008.
35. May BH, Lu C, Bennett L, Hügel HM and Xue CC: Evaluating the traditional Chinese literature for herbal formulae and individual herbs used for age-related dementia and memory impairment. Biogerontology 13: 299-312, 2012.
36. Goldar S, Khaniani MS, Derakhshan SM and Baradaran B: Molecular mechanisms of apoptosis and roles in cancer development and treatment. Asian Pac J Cancer Prev 16: 2129-2144, 2015.
37. Chen CT, Chen YC, Yamaguchi H and Hung MC: Carglumic acid promotes apoptosis and suppresses cancer cell proliferation in vitro and in vivo. Am J Cancer Res 5: 3560-3569, 2015.
38. Heath-Engel HM, Chang NC and Shore GC: The endoplasmic reticulum in apoptosis and autophagy: Role of the BCL-2 protein family. Oncogene 27: 6419-6433, 2008.
39. Yun SI, Yoon HY and Chung YS: Glycogen synthase kinase-3beta regulates etoposide-induced apoptosis via Bcl-2 mediated caspase-3 activation in C3H10T1/2 cells. Apoptosis 14: 771-777, 2009.
40. Kelm JM, Timmins NE, Brown CJ, Fussenegger M and Nielsen LK: Method for generation of homogeneous multicellular tumor spheroids applicable to a wide variety of cell types. Biotechnol Bioeng 83: 173-180, 2003.
41. Weiswald LB, Bellet D and Dangles-Marie V: Spherical cancer models in tumor biology. Neoplasia 17: 1-15, 2015.
42. Winters BS, Shepard SR and Foty RA: Biophysical measurement of brain tumor cohesion. Int J Cancer 114: 371-379, 2005.
43. López J, Poitevin A, Mendoza-Martínez V, Pérez-Plasencia C and García-Carrancá A: Cancer-initiating cells derived from established cervical cell lines exhibit stem-cell markers and increased radioresistance. BMC Cancer: Jan 28, 2012 (Epub ahead of print). doi: 10.1186/1471-2407-12-48.
44. Grinchuk OV, Motakis E and Kuznetsov VA: Complex sense-antisense architecture of TNFAIP1/POLDIP2 on 17q11.2 represents a novel transcriptional structural-functional gene module involved in breast cancer progression. BMC Genomics 11 (Suppl 1): S9, 2010.
45. Skoblov M, Marakhonov A, Marakasova E, Guskova A, Chandhoke V, Birerdinc A and Baranova A: Protein partners of KCTD proteins provide insights about their functional roles in cell differentiation and vertebrate development. Bioessays 35: 586-596, 2013.